Available online at www.sciencedirect.com
ScienceDirect
Renewable Energy 32 (2007) 2223–2241
RENEWABLE ENERGY
www.elsevier.com/locate/renene

Energy and exergy efficiencies of a hybrid photovoltaic–thermal (PV/T) air collector

Anand S. Joshi*, Arvind Tiwari

Centre for Energy Studies, Indian Institute of Technology Delhi, Hauz Khas, New Delhi 110016, India

Received 22 January 2006; accepted 21 November 2006
Available online 1 February 2007

Abstract

In this communication, an attempt has been made to evaluate exergy analysis of a hybrid photovoltaic–thermal (PV/T) parallel plate air collector for cold climatic condition of India (Srinagar). The climatic data of Srinagar for the period of four years (1998–2001) has been obtained from Indian Metrological Department (IMD), Pune, India. Based on the data four climatic conditions have been defined. The performance of a hybrid PV/T parallel plate air collector has been studied for four climatic conditions and then exergy efficiencies have been carried out. It is observed that an instantaneous energy and exergy efficiency of PV/T air heater varies between 55–65 and 12–15%, respectively. These results are very close to the results predicted by Bosanac et al. [Photovoltaic/thermal solar collectors and their potential in Denmark. Final Report, EFP Project, 2003, 1713/00-0014, www.solenergi.dk/rapporter/pvtpotentialindenmark.pdf].

Keywords: Exergy; Hybrid photovoltaic–thermal; Solar energy

1. Introduction

To evaluate the performance of a photovoltaic–thermal (PV/T) collector, the value of electricity versus the heat from the collector is important. The performance of a PV/T collector can be evaluated in terms of energy efficiency and exergy efficiency. Bosanac et al. defined energy efficiency as the total energy yield for a year [1]. The results are calculated from 1st law of thermodynamics and exergy efficiency as the total exergy yield per year,

*Corresponding author. Tel.: +91 98109 34365.
E-mail address: anandsj75@rediffmail.com (A.S. Joshi).

0960-1481/$ - see front matter © 2006 Published by Elsevier Ltd.
doi:10.1016/j.renene.2006.11.013

Nomenclature

A	area of module (m^2)
b	breadth (m)
C_a	specific heat of air (kJ/kg K)
dx	elemental length (m)
EVA	ethyl vinyl acrelate
h_T	heat transfer coefficient from back surface to air through tedlar (W/m^2 K)
h_{p1}	penalty factor due to presence of solar cell material, tedlar and EVA
h_{p2}	penalty factor due to presence of interface between tedlar and working fluid through absorber plate
$I(t)$	incident solar intensity (a function of time) on the inclined module surface (W/m^2)
I_{HB}	terrestrial beam solar radiation on a horizontal surface at ground level (W/m^2)
I_{HD}	diffuse solar radiation on horizontal surface at ground level (W/m^2)
I_{ON}	normal extra terrestrial solar radiation (W/m^2)
I_N	normal terrestrial solar radiation at the ground level (W/m^2)
K_1	perturbation factor (dimensionless)
K_2	background diffuse radiation (W/m^2)
m	air mass (dimensionless)
$\dot{m}_a$	rate of flow of air mass (kg/s)
n	day of the year starting from January 1
L	length of the PV module (m)
PV	photovoltaic
PV/T	photovoltaic–thermal
$\dot{Q}_u$	monthly thermal energy (W/m^2)
$\dot{q}_u$	rate of useful energy transfer (W/m^2)
$\dot{q}_{exergy}$	rate of exergy (W/m^2)
T	number of sunshine hours (h)
T_a	ambient temperature (°C)
T_{air}	temperature of flowing air (°C)
T_{airin}	inlet air temperature (°C)
T_{airout}	outlet air temperature (°C)
T_{bs}	back surface temperature of tedlar (°C)
T_c	temperature of solar cell (°C)
T_R	cloudiness/haziness factor (dimensionless)
T_0	reference ambient temperature (K)
ΔT	difference between the ambient temperature and collector outlet temperature
U_b	overall heat transfer coefficient from bottom to ambient (W/m^2 K)
U_L	overall heat transfer coefficient from solar cell to ambient through top and back surface of insulation (W/m^2 K)
U_t	overall heat transfer coefficient from solar cell to ambient through glass cover (W/m^2 K)
U_T	conductive heat transfer coefficient from solar cell to air through tedlar (W/m^2 K)

U_{tT}	overall heat transfer coefficient from glass to tedlar through solar cell ($W/m^2 K$)
U_{tair}	overall heat transfer coefficient from glass to ambient ($W/m^2 K$)

Greek Letters

α	atmospheric transmittance
α_c	absorptivity of solar cell
α_T	absorptivity of tedlar
β_c	packing factor of solar cell
θ_Z	zenith angle (°)
η_c	efficiency of solar cell
$\eta_{exergyov}$	overall exergy efficiency
η_o	electrical efficiency under standard test condition
η_{ov}	overall thermal efficiency
τ	transmitivity of glass cover

which is the part of energy that could theoretically be converted to work in an initial Carnot process. The results are calculated from the 2nd law of thermodynamics known as the exergy efficiency. According to Coventry, exergy (sometimes called availability) is defined as the maximum theoretical useful work obtainable from a system as it returns to equilibrium with the environment [2].

Jones and Underwood have studied the temperature profile of a photovoltaic (PV) module in non-steady-state conditions [3]. They conducted experiments for cloudy as well clear day condition for energy analysis. The carrier of thermal energy associated with the PV module can either be air or water. The integrated arrangement for utilizing thermal energy as well as electrical energy, with a PV module is referred to as the hybrid PV/T system.

The hybrid PV/T system can be used for:

(i) Air heating [4–12] and
(ii) Water heating [6,13–19].

Performance of a PV/T system can be carried out either in terms of energy or exergy. Chow has analyzed the PV/T water collector with a single glazing in transient conditions, consisted of tubes, in thermal contact with the flat plate on account of metallic bond [16]. It has been observed that the electrical efficiency (the ratio of maximum power to the incident solar radiation) is increased by 2% at a mass flow rate of 0.01 kg/s due to decrease in temperature of solar cell of PV module and a plate to bond heat transfer coefficient $10^4 W/m^2 K$ with an addition thermal energy efficiency of 60%. Huang et al. have experimentally analyzed unglazed integrated photovoltaic–thermal solar system (IPVTS) for water heating under natural mode of operation [20]. They observed that the primary energy-saving efficiency of the IPVTS exceeds 0.60, which is higher than that for a conventional solar water heater or pure PV system. Kalogirou has observed the monthly performance of a glazed hybrid PV/T system under forced mode of operation for the climatic condition of Cyprus [14]. He observed an

increase of the mean annual efficiency of the PV solar system from 2.8% to 7.7% with an associated thermal energy efficiency of 49%. A similar study has also been made by Zondag et al. [13]. They have referred to a hybrid PV/T as a combi-panel, which converts solar energy into both electrical and thermal energy. The efficiency of the combi-panel was reported as 6.7% (electrical) and 33% (thermal energy), respectively.

Sandnes and Rekstad have studied the performance of a combined PV/T collector, which was constructed by pasting single crystal silicon cells onto a black plastic solar heat absorber (unglazed PV/T system) [18]. They recommended that the combined PV/T concept must be used for low-temperature thermal applications and for increasing the electrical efficiency of the PV system. Zakharchenko et al. have also studied unglazed hybrid PV/T systems with a suitable thermal contact between the panel and the collector [17]. To operate a PV module at low temperature, PV module should cover the low temperature part of the collector (e.g. at cold water inlet portion). Further, an unglazed hybrid PV/T system with a booster diffuse reflector was integrated with the horizontal roof of a building by Tripanagnostopoulos et al. [6]. They concluded that a PV/T system with a reflector yields distinctly clearly higher electrical and thermal energy output. They have studied the performance characteristic of a PV/T-water as well as a PV/T air system. An overall heat loss coefficient (U) and the thermal energy gain factor (g) for a combination of a ventilated vertical PV module and a double glazed window (PV facades) have derived by Infield et al. [5]. It is observed that the ventilated facades lead to enhancement of the electrical efficiency of a PV module on account of corresponding low temperature (generally below 45 °C). Hagazy and Sopian et al. investigated a glazed PV/T air system with a single or double pass air heater for space heating and drying [4,21]. They have developed thermal models for each system. The thermal energy, obtained from the glazed PV/T system gets increased along with lower electrical efficiency (due to high operating temperature). Further, Coventry has made an attempt to study the performance of a concentrating PV/T solar collector and concluded that overall thermal and electrical efficiencies of a PV/T concentrating system are 58% and 11%, respectively [22]. This gives a total energy efficiency of the system as 69%.

Little work has been carried out for exergy analysis of PV/T air/water heaters. Recently Bosanac et al. [1] have briefly carried out exergy analysis of PV/T system and reported that maximum exergy efficiency of PV/T system is about 12% against an overall maximum energy efficiency of 60%. Coventry and Lovehrove have also studied the exergy analysis of PV/T water system and reported that energy to exergy ratio of electrical and thermal are 1 and 16.8, respectively [2].

In this paper, an attempt has been made to study the exergy efficiency of unglazed PV/T air heating module for the cold and cloudy condition of Srinagar.

1.1. Hybrid PV/T air collector

Fig. 1a shows the schematic diagram of a PV/T air collector. Air has been considered as the medium for transport of thermal energy. Two PV modules with an effective area of 0.61 m^2 each are connected in series. The module has been mounted on a wooden structure with the air duct below the module known as tedlar. In other words tedlar is an insulating and non-corrosive material used beneath the solar cell for better support to PV module.

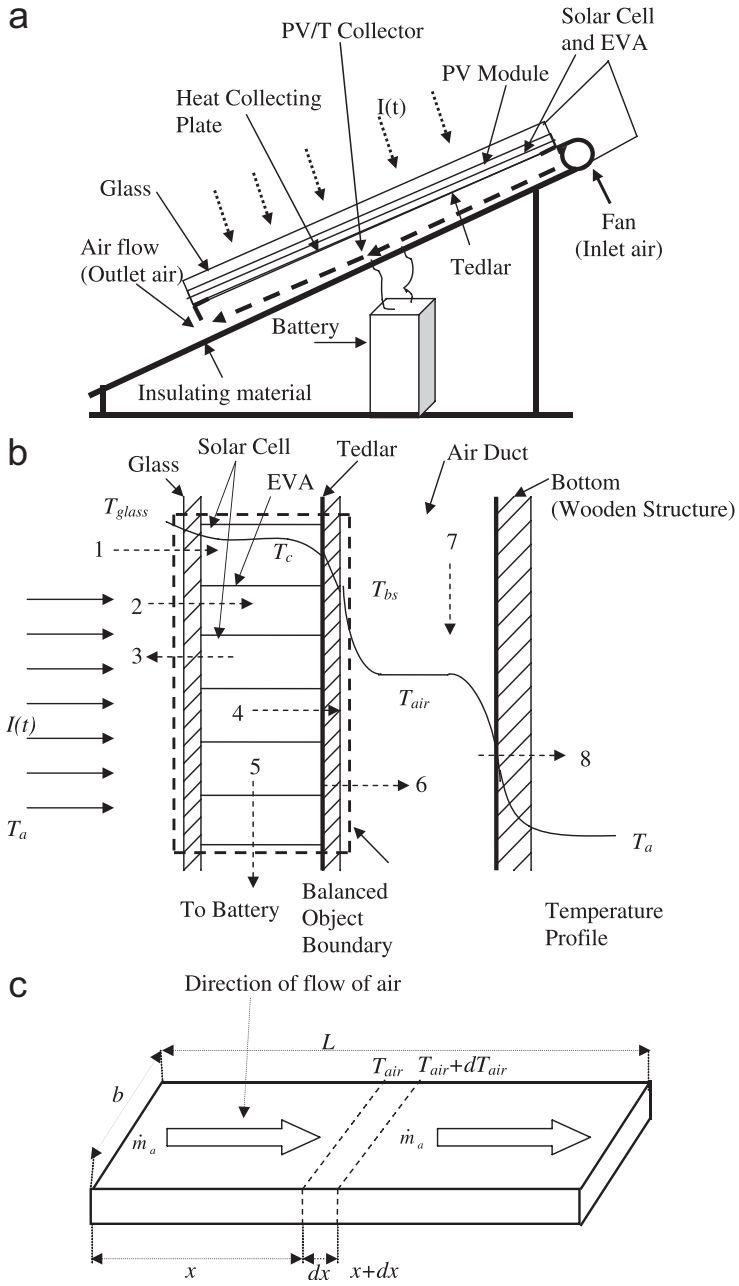

Fig. 1. (a) Schematic diagram of integrated PV/T system (IPVTS) when air is used as the medium to collect thermal energy. (b) Cross-sectional view (rotated at 90° from horizontal) of hybrid PV/T air collector with temperature profile. (c) An elemental length 'dx' shows flow pattern of air below tedlar.

Table 1
Design parameters for integrated photovoltaic thermal system with air as the heat removal medium [12]

Parameters	Values	Parameters	Values
A	0.61 m^2	U_b	0.62 W/m^2 K
B	0.45 m	U_t	2.8 W/m^2 K
h_{p1}	0.88	U_{tT}	8.11 W/m^2 K
L	1.2 m	U_T	66 W/m^2 K
β_c	0.83	α_c	0.90
η_c	0.12	α_T	0.50
τ	0.95	h_T	6.5 W/m^2 K

There is a provision for inlet and outlet air to flow through the duct. The PV module with a wooden structure is placed on a steel frame.

The design parameters of hybrid PV/T system are given in Table 1.

2. Methodology

2.1. Evaluation of solar radiation

The data of global radiation and diffuse radiation are obtained from Indian Metrological Department (IMD) Pune, India for the years 1991–2001. Singh and Tiwari has defined the day of the year for four different weather conditions in terms of number of sunshine hours and ratio of daily diffuse to daily global radiation as described below [23]:

(a) Clear day (blue sky): The ratio of daily diffuse to daily global radiation less then or equal to 0.25 and number of sunshine hours greater then or equal to 9 h.

(b) Hazy day (fully): The ratio of daily diffuse to daily global radiation between 0.25 and 0.50 and number of sunshine hours between 7 and 9 h.

(c) Hazy and cloudy (partially): The ratio of daily diffuse to daily global radiation between 0.5 and 0.75 and number of sunshine hours between 5 and 7 h.

(d) Cloudy day (fully): The ratio of daily diffuse to daily global radiation greater then or equal to 0.75 and number of sunshine hours less then or equal to 5 h.

The average values of global and diffuse radiation on horizontal surface for each case and month are given in Tables 2 and it has been used to evaluate cloudiness/haziness and atmospheric transmittances [23]. The results are given in Table 3 for all the four type of days.

The values of Table 3 has been used to calculate beam and diffuse radiation on horizontal surface for each case and month by using the following equation [23]:

$$I_{HB} = I_{ON} \exp[-(m\varepsilon T_R + \alpha)] \cos(\theta_Z) = I_N \cos(\theta_Z), \quad (1)$$

where I_{HB} is terrestrial beam solar radiation at ground level in W/m^2, I_{ON} is normal extra terrestrial beam solar radiation in W/m^2, m, air mass (dimensionless) is the ratio of optical

Table 2
Average hourly global (Ig) and diffuse (Id) radiation (W/m^2) for the months of January–December (IMD)

Radiation	Time	Month											
		Jan	Feb	Mar	Apr	May	June	July	Aug	Sep	Oct	Nov	Dec
Type a													
Global	8am	73.61	69.79	221.53	373.06	408.52	434.92	408.89	289.58	291.25	179.42	66.67	30.55
	9am	252.78	284.72	461.57	594.31	633.52	634.52	626.11	542.71	492.78	379.32	272.22	213.89
	10am	455.56	481.60	665.74	776.53	793.52	796.43	788.06	711.11	668.47	544.75	452.78	360.19
	11am	545.84	647.22	800.70	880.56	915.74	904.76	888.89	831.60	784.30	661.83	558.33	485.19
	12pm	577.78	732.99	891.43	932.50	981.67	951.19	950.28	885.42	842.71	719.34	652.78	543.52
	1pm	572.22	747.57	905.79	931.81	975.74	963.89	958.89	903.47	832.57	702.06	622.22	513.89
	2pm	511.11	688.20	841.67	870.70	913.70	919.84	850.55	843.75	760.69	622.53	563.89	470.37
	3pm	418.06	562.50	703.71	735.69	783.89	795.24	727.78	745.49	612.71	479.84	380.56	362.04
	4pm	227.78	356.60	498.15	531.11	560.56	626.19	550.55	534.38	400.49	290.84	216.67	201.85
	5pm	43.06	127.08	245.37	283.06	344.81	417.46	317.78	293.40	196.11	94.86	25.00	52.78
Diffuse	8am	19.45	45.48	74.31	99.03	104.26	102.78	119.72	106.60	89.31	61.63	33.33	2.78
	9am	70.83	111.46	105.32	122.92	129.63	125.79	151.11	128.82	121.87	95.68	108.33	29.63
	10am	101.39	112.50	123.38	138.47	145.56	139.29	164.17	125.35	138.47	113.89	158.33	61.11
	11am	115.28	127.78	143.52	152.08	152.59	130.56	176.39	133.68	147.15	131.28	172.22	85.18
	12pm	119.44	136.46	153.70	156.25	151.30	135.32	166.94	127.08	149.86	137.14	136.11	94.44
	1pm	118.06	134.72	144.91	150.97	147.22	132.14	152.78	127.08	142.29	125.21	127.78	112.96
	2pm	118.06	113.19	132.64	143.75	147.41	121.43	144.72	116.67	127.36	104.42	77.78	105.55
	3pm	84.72	95.14	120.37	142.50	134.44	121.03	140.56	107.64	108.54	84.67	58.33	95.37
	4pm	48.61	77.08	90.74	130.83	134.45	111.51	130.28	100.69	90.00	58.44	33.33	83.33
	5pm	18.06	44.79	62.04	95.00	109.45	88.49	100.28	78.13	60.00	26.13	22.22	20.37
	8am	25.70	86.11	146.43	266.88	359.83	366.03	316.58	267.13	250.82	168.98	46.20	33.33
Type b													
Global	9am	165.51	250.00	369.05	464.96	547.76	572.49	555.69	538.89	463.40	364.82	184.35	202.78
	10am	315.05	474.31	556.75	676.28	733.98	755.88	713.58	671.29	636.77	525.00	339.72	277.78
	11am	421.53	719.44	661.51	826.92	857.91	919.23	892.03	864.82	742.16	639.58	462.50	341.67
	12pm	463.66	812.50	769.05	858.55	893.16	878.53	888.80	899.08	761.93	693.06	518.52	525.00
	1pm	473.38	811.81	816.67	811.32	880.66	888.94	844.88	800.82	761.44	677.78	521.20	544.44
	2pm	457.18	750.00	665.87	673.29	711.65	808.60	769.77	730.93	694.77	593.29	473.89	491.67
	3pm	361.81	585.41	535.72	446.37	355.13	542.84	590.17	637.50	527.29	448.61	357.59	327.78
	4pm	216.43	359.03	351.98	390.17	318.70	419.07	438.24	457.41	334.80	266.43	203.52	155.56
	5pm	52.55	70.83	184.53	184.83	206.31	222.60	258.29	293.98	157.35	81.25	58.80	27.78
Diffuse	8am	17.13	56.95	54.36	108.76	125.94	128.11	143.91	159.72	124.02	86.34	27.13	8.33
	9am	87.27	129.86	121.82	166.88	191.72	200.37	203.20	206.02	167.98	139.82	97.59	91.67
	10am	124.77	231.25	196.43	204.91	256.89	264.56	253.81	243.06	196.73	168.98	143.61	133.33
	11am	148.84	235.41	226.59	213.25	300.27	321.73	278.92	236.11	222.06	194.68	166.67	138.89
	12pm	162.73	226.39	267.46	238.67	312.61	307.48	265.32	223.15	213.24	203.93	182.78	197.22
	1pm	160.88	206.25	223.41	284.62	308.23	311.13	267.14	223.15	215.36	203.24	183.89	175.00
	2pm	151.62	192.36	223.41	261.54	249.08	283.01	232.25	181.48	199.84	185.19	161.67	158.33
	3pm	110.19	150.00	212.70	186.54	124.30	190.00	195.69	201.39	173.69	146.53	127.78	133.33
	4pm	78.24	111.11	170.63	170.51	111.54	146.67	161.95	177.22	131.05	102.78	77.31	61.11
	5pm	23.61	48.61	96.43	91.88	72.21	77.91	87.10	96.30	79.57	40.28	17.96	11.11
Type c													
Global	8am	23.89	35.48	51.39	208.33	204.34	204.85	188.89	177.43	165.97	133.33	33.33	39.75
	9am	90.00	123.89	94.44	352.08	360.42	217.52	344.44	320.135	295.83	211.11	155.56	158.48
	10am	191.67	230.67	151.39	592.36	474.48	323.26	372.22	387.85	403.48	258.33	289.81	238.50
	11am	271.67	338.09	281.94	622.22	550.35	380.51	505.56	532.64	559.72	427.78	399.38	295.91

Table 2 (*continued*)

Radiation	Time	Month											
		Jan	Feb	Mar	Apr	May	June	July	Aug	Sep	Oct	Nov	Dec
	12pm	306.67	399.70	434.72	783.34	668.76	447.54	541.67	529.165	516.66	702.78	428.70	304.76
	1pm	377.78	396.53	408.33	603.47	651.74	574.04	711.11	622.22	533.33	636.11	400.00	242.92
	2pm	359.44	392.25	475.00	604.86	600.35	600.71	577.78	559.725	541.67	433.33	367.28	260.59
	3pm	383.33	321.33	390.28	576.39	574.99	500.37	508.33	443.055	377.78	202.78	255.86	169.61
	4pm	155.56	157.83	226.38	331.25	284.38	293.83	263.89	290.28	316.67	94.44	124.69	88.34
	5pm	30.00	38.83	61.11	188.89	229.34	268.86	225.00	180.21	135.42	50.00	32.10	23.85
Diffuse	8am	19.89	23.26	25.00	153.47	141.97	130.48	55.56	97.64	139.72	100	24.07	25.00
	9am	73.34	79.75	44.44	228.47	183.51	138.55	91.67	144.79	197.92	147.22	100.62	99.67
	10am	148.33	124.97	63.89	325.00	265.45	205.90	238.89	271.88	304.86	258.33	143.83	150.00
	11am	201.66	164.23	80.56	375.00	308.68	242.36	219.44	296.52	373.61	350.00	187.35	186.11
	12pm	257.22	227.73	166.67	355.56	320.31	285.06	308.33	331.6	354.86	372.22	243.52	191.67
	1pm	281.11	261.95	288.89	423.61	394.62	365.63	427.78	389.93	352.08	386.11	238.89	152.78
	2pm	212.78	258.06	363.89	313.19	347.91	382.62	385.56	352.5	319.44	316.67	227.78	163.89
	3pm	160.00	217.78	372.22	277.78	298.24	318.71	346.11	309.51	272.92	191.67	169.45	106.67
	4pm	76.67	96.25	113.89	226.39	206.77	187.15	211.11	235.07	259.03	94.44	97.22	55.56
	5pm	18.33	35.29	72.22	115.28	143.26	171.25	202.78	154.31	105.83	41.67	25.31	15.00
Type d													
Global	8am	29.63	56.95	77.78	127.78	177.78	186.11	194.44	163.89	41.67	39.45	37.22	25.00
	9am	148.15	168.06	205.56	241.67	277.78	263.89	250.00	191.67	100.00	129.16	158.33	112.22
	10am	258.89	279.17	369.44	394.44	419.44	369.44	319.44	449.44	219.44	294.44	369.44	225.00
	11am	351.85	286.81	391.67	188.89	489.45	511.39	533.33	544.44	438.89	406.94	375.00	438.89
	12pm	361.11	364.58	366.67	550.00	733.33	611.11	488.89	688.33	641.67	527.78	413.89	531.11
	1pm	300.00	323.61	283.33	933.33	933.33	708.33	483.33	593.89	575.00	483.33	391.67	491.67
	2pm	286.11	287.50	283.33	583.33	883.33	655.55	427.78	569.44	491.67	405.56	319.44	388.89
	3pm	171.30	221.53	200.00	427.78	655.56	590.28	325.00	375.00	341.67	312.50	283.33	304.44
	4pm	80.56	100.00	144.44	119.44	94.44	184.72	275.00	197.22	277.78	188.89	100.00	105.56
	5pm	20.37	42.36	47.22	77.78	108.34	141.67	175.00	116.67	88.89	60.56	32.22	16.67
Diffuse	8am	25.48	46.53	67.67	98.39	129.11	158.19	180.56	137.67	38.89	36.11	33.33	21.00
	9am	127.41	147.92	178.84	186.09	193.34	224.31	238.89	161.00	97.22	123.33	129.44	107.22
	10am	222.65	243.75	321.41	303.72	286.03	314.02	313.89	377.53	216.67	256.94	297.22	213.89
	11am	302.59	258.33	340.75	145.45	439.25	434.68	363.89	457.33	406.11	352.22	298.33	336.89
	12pm	310.55	260.42	246.50	423.50	600.50	519.44	441.67	578.2	507.78	415.83	323.89	350.00
	1pm	258.00	293.75	190.91	718.66	779.41	602.08	462.78	498.87	501.67	380.00	258.33	350.00
	2pm	246.05	258.33	319.00	449.16	579.32	557.22	416.67	478.33	488.89	358.61	228.33	230.00
	3pm	147.32	184.03	246.50	329.39	412.28	501.74	322.22	315.00	338.89	256.06	173.22	258.89
	4pm	69.28	88.19	125.66	91.97	58.28	157.01	272.22	165.66	230.56	163.89	97.22	100.56
	5pm	17.52	38.20	41.08	59.89	78.70	120.42	172.22	98.00	86.11	57.77	29.44	13.89

thickness of atmosphere (ε) at a specific point in time to the optical thickness of atmosphere when sun is at zenith, θ_Z is zenith angle in degree and I_N is normal terrestrial solar radiation at ground level in W/m^2 and

$$I_{HD} = K_1(I_{ON} - I_N)\cos(\theta_Z) + K_2, \tag{2}$$

where I_{HD} is terrestrial diffuse solar radiation on horizontal surface at ground level in W/m^2, T_R is cloudiness/haziness factor (dimensionless), α is atmospheric transmittance, K_1

Table 3
Parameters of Joshi and Tiwari on horizontal surface for sunshine hours = 10 for all four type of days

Type of day	Parameters	Month											
		Jan	Feb	Mar	Apr	May	June	July	Aug	Sep	Oct	Nov	Dec
a	T_R	1.45	5.37	3.31	4.25	5.41	3.63	5.77	6.45	4.06	2.61	4.03	0.72
	α	0.33	−0.36	−0.03	−0.03	−0.12	0.08	−0.09	−0.23	0.03	0.20	−0.37	0.53
	K_1	0.37	0.63	0.69	0.37	0.51	0.33	0.17	0.37	0.46	0.43	0.66	0.33
	K_2	−6.14	−82.86	−94.01	−10.95	−79.57	−13.73	68.06	−42.79	−60.27	−47.83	−37.00	−6.60
b	T_R	3.09	6.98	4.65	6.92	5.86	6.82	7.40	7.58	6.41	4.04	0.04	0.35
	α	0.38	−0.48	0.23	0.06	0.29	0.11	0.00	−0.13	−0.04	0.19	1.16	1.00
	K_1	0.39	0.83	0.59	0.42	0.32	0.63	0.48	0.38	0.48	0.52	0.37	0.41
	K_2	−23.08	−110.23	−107.74	−49.61	0.26	−167.86	−80.06	−13.91	−66.64	−62.52	−14.63	−12.20
c	T_R	2.35	6.59	6.31	7.57	8.69	8.00	9.72	8.23	7.36	5.02	1.86	0.76
	α	1.64	0.86	1.35	0.57	0.61	0.81	0.69	0.90	0.99	1.49	1.47	1.98
	K_1	0.41	0.42	0.48	0.54	0.50	0.39	0.56	0.49	0.44	0.52	0.41	0.31
	K_2	−37.87	−85.68	−180.45	−120.38	−146.97	−87.44	−228.91	−147.96	−62.10	−93.64	−40.07	−12.15
d	T_R	1.69	1.36	7.52	9.09	9.48	10.79	10.93	8.54	8.16	7.75	3.78	2.44
	α	2.63	2.97	1.87	1.35	1.13	1.56	3.08	1.71	3.15	1.70	1.74	2.04
	K_1	0.43	0.36	0.35	0.62	0.92	0.80	0.45	0.75	0.67	0.55	0.48	0.63
	K_2	−41.27	−44.68	−65.17	−254.24	−467.30	−421.63	−129.49	−356.92	−261.85	−119.53	−49.16	−64.02

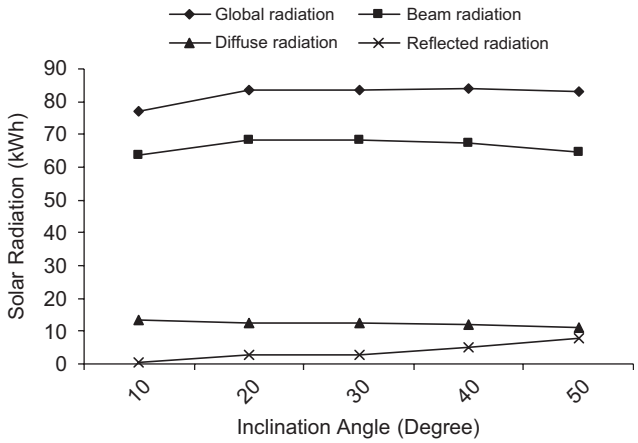

Fig. 2. The variation of annual solar radiation for clear day with inclination.

is perturbation factor (dimensionless) and K_2 is background diffuse radiation (W/m^2).The values of T_R, α, K_1 and K_2 for each case and month have been given in Table 3.

The beam and diffuse radiation on horizontal surface obtained from Eqs. (1) and (2) are converted on an inclined PV/T module by using Liu and Jordan formula for optimized inclination [24,25]. The variation of annual solar radiation for clear day with inclination is shown in Fig. 2. It is seen that the maximum solar energy is available for 30–40° inclination and hence the optimum inclination has been used to evaluate energy and exergy analysis of PV/T system.

2.2. Thermal modeling of the hybrid PV/T air collector

In order to write the energy balance equation for each component of a PV/T air collector as shown in the Fig. 1b, the following assumptions have been made:

(i) The system is in quasi-steady-state condition.
(ii) The transmittivity of EVA is approximately 100 percent.
(iii) The temperature variation along the thickness is negligible.
(iv) The airflow through duct is uniform for the forced mode of operation for streamline flow and
(v) The PV/T module in inclined at average optimum value of 35^0, which is about equal to latitude of Srinagar.

2.3. Energy balance

Referring to Figs. 1a and b and following [12], the energy balance equations are as follows:

For the PV module:

$$\underset{1}{\tau\left[\alpha_c I(t)\beta_c + \left(1-\beta_c\right)\alpha_T I(t)\right]bdx} = \underset{2}{[U_t(T_c - T_a)} + \underset{3}{U_T(T_c - T_{bs})]bdx} + \underset{4}{\eta_c I(t)\beta_c bdx}. \quad \underset{5}{} \tag{3}$$

Five elements of the Eq. (3) can be described as

1 the rate of solar energy received by solar cell after transmission;
2 the rate of solar energy absorbed by tedlar after transmission from EVA;
3 the rate of heat lost from solar cell to ambient through glass cover;
4 the rate of heat lost from solar cell to back surface of the tedlar for elemental area '*bdx*' and
5 the rate of electrical energy available from solar cell of PV module.

For the back surface of the Tedlar:

Energy balance for back surface of the tedlar is as follows:

$$\underset{4}{U_T(T_c - T_{bs})bdx} = \underset{6}{h_T(T_{bs} - T_{air})bdx}, \tag{4}$$

where

6 the rate of heat transfer from back surface to flowing air for elemental area '*bdx*'.

For the air flowing below the tedlar (air duct, Figs. 1b and c):

$$\underset{6}{h_T(T_{bs} - T_{air})bdx} = \underset{7}{\dot{m}_a C_a (dT_{air}/dx)\,dx} + \underset{8}{U_b(T_{air} - T_a)bdx}, \tag{5}$$

where
7 the heat carried away with the flowing air and
8 the rate of heat transfer from flowing air to ambient for elemental area 'bdx'

An expression for the temperature of the flowing air below the tedlar can be obtained by integrating Eq. (5) with the initial condition $T_{air} = T_{airin}$, at $x = 0$ as

$$T_{air} = \frac{h_{p1}h_{p2}(\alpha\tau)_{eff}I(t)}{U_L}\left(1 - e^{\frac{-bU_L}{\dot{m}_a c_a}x}\right) + T_a\left(1 - e^{\frac{-bU_L}{\dot{m}_a c_a}x}\right) + T_{airin}e^{\frac{-bU_L}{\dot{m}_a c_a}x}. \quad (6)$$

Eq. (6) can be used to get average air temperature and then solar cell and the back surface temperature from Eqs. (3) and (4), respectively.

The outlet air temperature (T_{airout}) of the flowing air below the tedlar can be obtained from the above equation as

$$T_{airout} = T_{air}\Big|_{x=L}\left[\frac{h_{p1}h_{p2}(\alpha\tau)_{eff}I(t)}{U_L} + I(t)\right]\left(1 - e^{\frac{-bU_L}{\dot{m}_a c_a}L}\right) + T_{airin}e^{\frac{-bU_L}{\dot{m}_a c_a}L}. \quad (7)$$

The rate of useful thermal energy obtained from the PV/T air collector is thus obtained as [12]

$$\dot{q}_u = \dot{m}_a c_a(T_{airout} - T_{airin}) = \frac{\dot{m}_a c_a}{U_L}\left\{h_{p1}h_{p2}(\alpha\tau)_{eff}I(t) - U_L(T_{airin} - T_a)\right\}\left(1 - e^{\frac{-bU_L}{\dot{m}_a c_a}L}\right), \quad (8)$$

Table 4
The average number of days in different months under different weather types for Srinagar climatic condition

Type of day	Jan	Feb	Mar	Apr	May	June	July	Aug	Sep	Oct	Nov	Dec
a	2	7	9	10	17	14	10	10	14	9	5	3
b	15	10	10	13	9	10	10	9	8	8	12	8
c	12	9	9	6	4	5	7	9	5	9	10	19
d	2	2	3	1	1	1	1	3	3	3	3	1

Table 5
Average ambient temperature (°C) at Srinagar for January–December (IMD)

Time	Jan	Feb	Mar	Apr	May	June	July	Aug	Sep	Oct	Nov	Dec
8am	−2.0	2.8	6.3	15.6	16.1	21.0	21.1	19.3	17.2	6.4	1.5	1.8
9am	−2.2	2.8	4.8	15.0	15.6	20.8	20.8	18.9	16.7	6.0	1.0	1.9
10am	−2.2	2.5	4.0	14.3	15.1	20.3	20.3	18.1	16.0	6.0	0.5	1.7
11am	−2.4	2.5	4.3	14.3	15.8	20.6	20.3	18.1	15.7	6.0	0.5	1.6
12pm	−2.3	2.5	4.8	14.3	17.6	22.7	20.4	18.3	17.0	6.5	1.0	1.7
1pm	−2.1	2.5	7.2	15.0	20.8	25.2	22.9	20.6	20.9	10.4	3.0	1.0
2pm	−1.6	3.4	7.6	15.0	21.8	26.0	25.0	23.0	23.8	13.9	6.0	2.7
3pm	−1.6	5.3	10.1	15.1	25.3	26.7	25.5	25.2	25.9	17.0	8.3	4.7
4pm	−0.6	5.5	9.9	17.1	26.4	28.6	27.3	26.7	27.4	19.4	10.5	6.5
5pm	−0.2	7.5	10.8	17.0	27.8	30.1	28.1	27.6	28.8	21.9	11.5	8.4

where $U_L = U_{tair} + U_b$, $h_{p1} = U_T/(U_t + U_T)$, is the penalty factor due to the glass cover of a PV module, and $h_{p2} = h_T/(U_{tT} + h_T)$, is the penalty factor due to the tedlar of a PV module,

$$(\alpha\tau)_{eff} = \tau\{\alpha_c\beta_c + \alpha_T(1-\beta_c) - \eta_c\beta_c\}I(t).$$

Following Bosanac et al. the rate of exergy obtained from the PV/T air collector is thus obtained as [1]

$$\dot{q}_{exergy} = \dot{q}_u\left[1 - \frac{(T_0 + 273)}{293 + \Delta T}\right], \tag{9}$$

where T_0 is the reference ambient temperature = 20 °C (293 K) and ΔT is the difference between the ambient temperature and the collector outlet temperature.

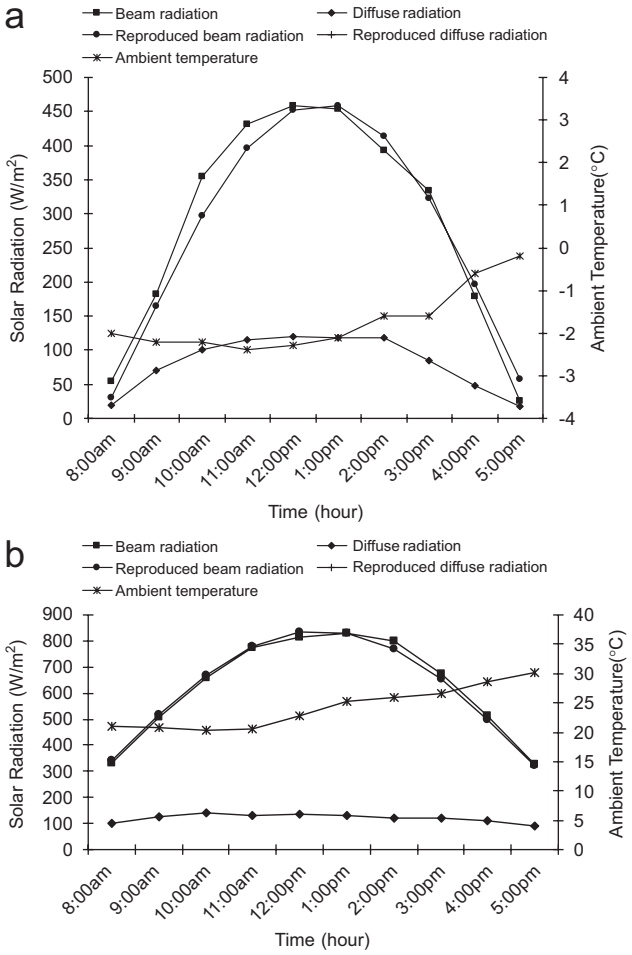

Fig. 3. (a) Reproduced beam and diffuse radiation with ambient temperature for January at Srinagar. (b) Reproduced beam and diffuse radiation with ambient temperature for June at Srinagar.

The equivalent rate of thermal energy for conversion factor of 0.38 for thermal power plant of PV module will be as follows:

$$\dot{q}_{\text{eth}} = \frac{\eta_0\{1-\beta\Delta T\}I(t)bL}{0.38}. \tag{10}$$

Here $\beta = 0.0045$ per °C.

The overall efficiency of the PV/T collector is [12]

$$\eta_{\text{ov}} = \frac{\sum_{i=1}^{T}\left[\dot{q}_{\text{eth}} + \dot{q}_{\text{u}}\right]}{\sum_{i=1}^{T} I(t)bL}, \tag{11}$$

where T is the sunshine hours.

Eq. (11) can also be written as

$$\eta_{\text{ov}} = \frac{\eta_{\text{o}}\{1-\beta\Delta T\}}{0.38} + \eta_{\text{th}}. \tag{12}$$

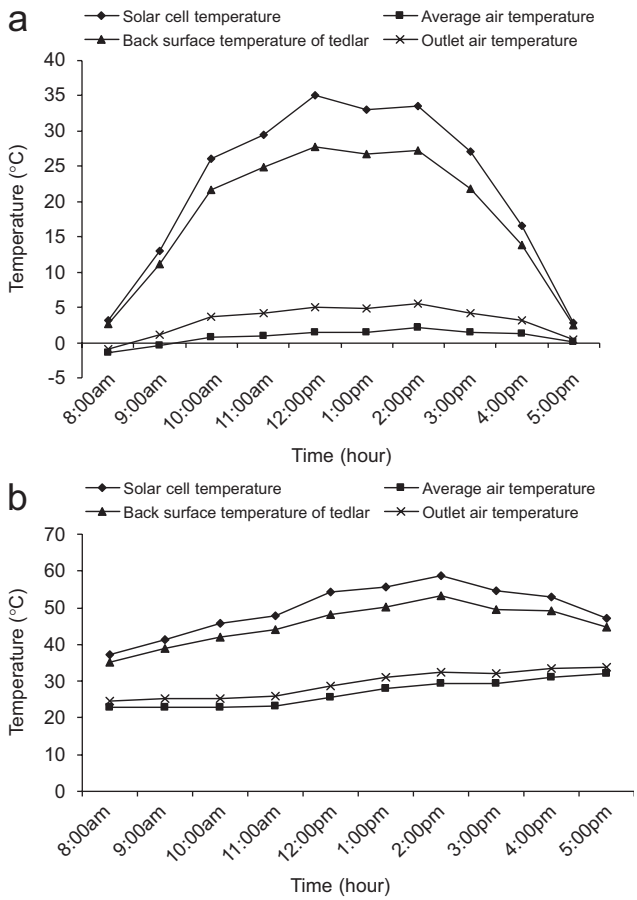

Fig. 4. (a) Predicted temperatures (°C) for a PV/T system in January at Srinagar. (b) Predicted temperatures (°C) for a PV/T system in June at Srinagar.

The exergy efficiency of The PV/T air collector will be determined as

$$\eta_{\text{exergyov}} = \eta_{\text{o}}[1 - \beta\Delta T] + \eta_{\text{th}}\left[1 - \frac{(T_0 + 273)}{293 + \Delta T}\right], \tag{13}$$

The monthly thermal energy and exergy have been evaluated by using the data of Tables 4 and 5 for all cases are as follows:

$$\dot{Q}_{\text{u}} = \sum_{i=1}^{4} n_i \dot{q}_{\text{u}i}. \tag{14}$$

Here $\dot{q}_{\text{u}i}$ can be evaluated from Eq. (8) for each case for given n_i for each month. i stands for type of the days in month (e.g. $i = 1$ means 'a' type weather condition, $i = 2$ means 'b' type weather condition). Similarly monthly exergy can be obtained [26]. The yearly thermal energy and exergy can be evaluated by summing monthly thermal energy and exergy.

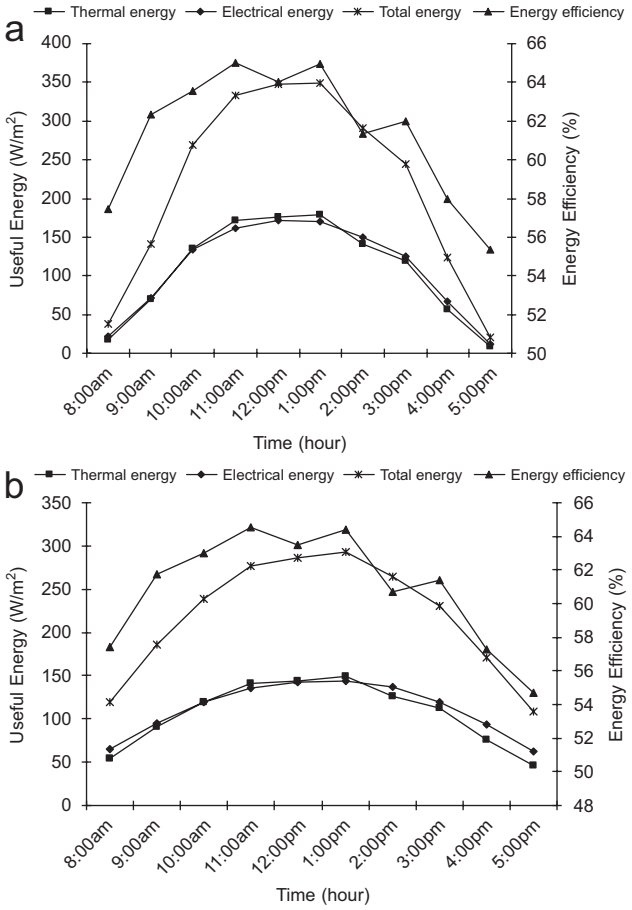

Fig. 5. (a) Useful thermal, electrical and total energy (W/m^2) and energy efficiency for January at Srinagar. (b) Useful thermal, electrical and total energy (W/m^2) and energy efficiency for June at Srinagar.

3. Numerical results

Eqs. (1) and (2) have been used to evaluate the beam and diffuse radiation for all cases and each month by using the parameters of Table 3. The hourly variation of beam and diffuse radiation and ambient temperature for typical day for January and June for case (a) has been shown in Figs. 3. The total radiation on inclined PV module is obtained by using Liu and Jordon formula. The average data of total and diffuse radiation given in Table 2a is used to determine the beam radiation and the parameters of Table 3 are used to reproduce the average beam and diffuse radiation for the month of January and June and are shown in Figs. 3. The beam radiation varies from a minimum value of 50 W/m^2 at 8 am and 5 pm to a maximum value of 450 W/m^2 at 12 pm for the month of January (Fig. 3a) where as it varies from a minimum value of 320 W/m^2 at 8 am and 5 pm to a maximum value of 820 W/m^2 at 12 pm for the month of June (Fig. 3b).

Eqs. (3–6) have been used to evaluate the hourly variation of average air, solar cell, back surface and outlet air temperatures for typical day for the month of January and June and

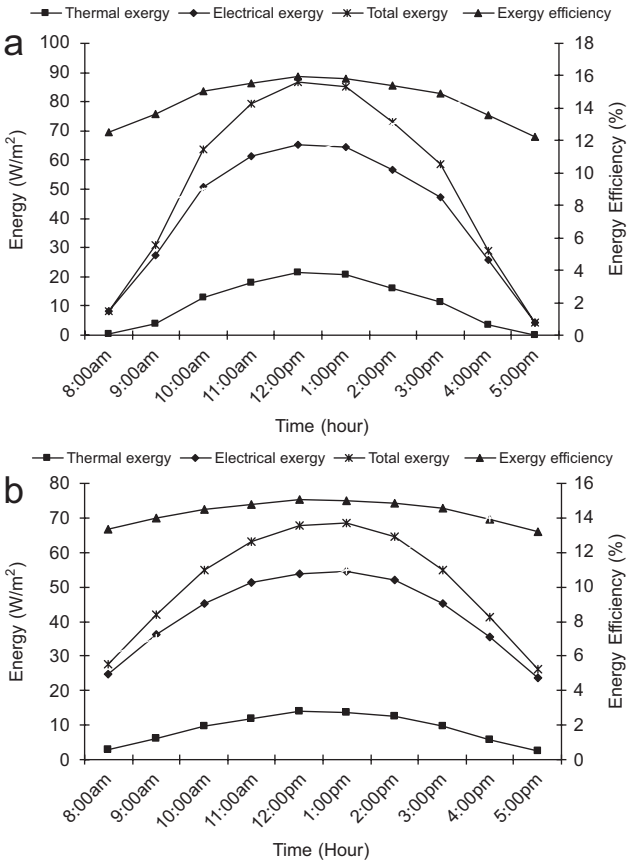

Fig. 6. (a) Electrical, thermal and total exergy and exegy efficiency for January at Srinagar. (b) Electrical, thermal and total exergy and exegy efficiency for June at Srinagar.

the results have been shown in Figs. 4. Computations were carried out for climatic data of Figs. 3 and design parameters of Table 1. It is observed that there is significant increase in outlet air temperature which gives an additional thermal energy in addition to electrical energy for both winter and summer climatic conditions. The average air temperature is slightly lower than outlet air temperature as expected. The solar cell and back surface temperature is significantly higher than the outlet air temperature. The outlet air temperature can be further increased by reducing flow velocity of air in duct.

Eqs. (8,11,12 and 13) have been used for evaluating the hourly useful energy and exergy and corresponding energy and exergy efficiencies and its hourly variation have been shown in Figs. 5 and 6, respectively. It is evident that there is variation of energy efficiency between 55% and 65%. The total energy varies from a minimum value of

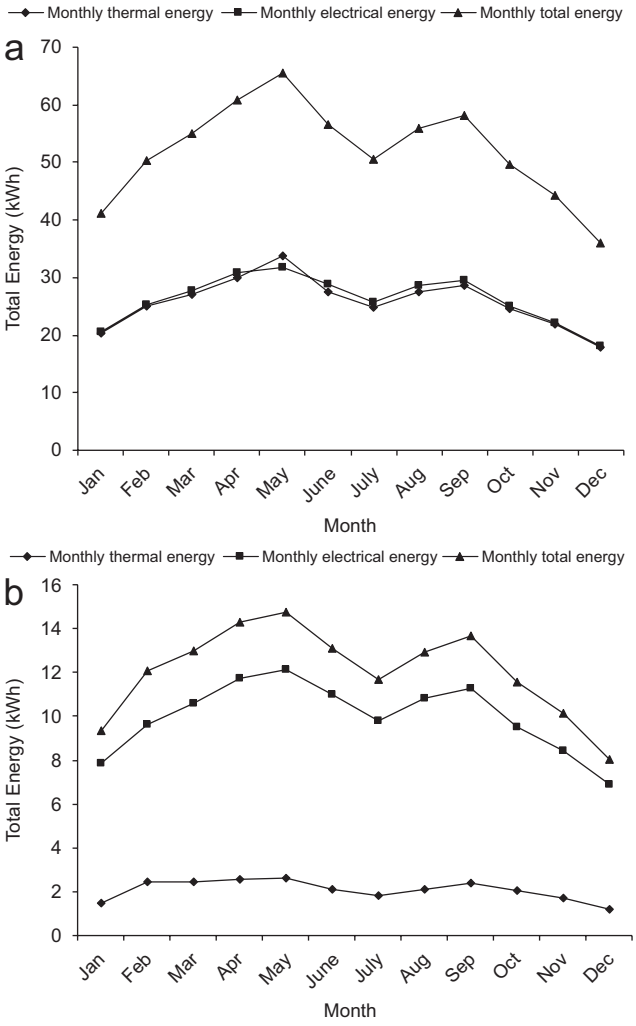

Fig. 7. (a) Monthly total energy analysis for Srinagar. (b) Monthly total exergy analysis for Srinagar.

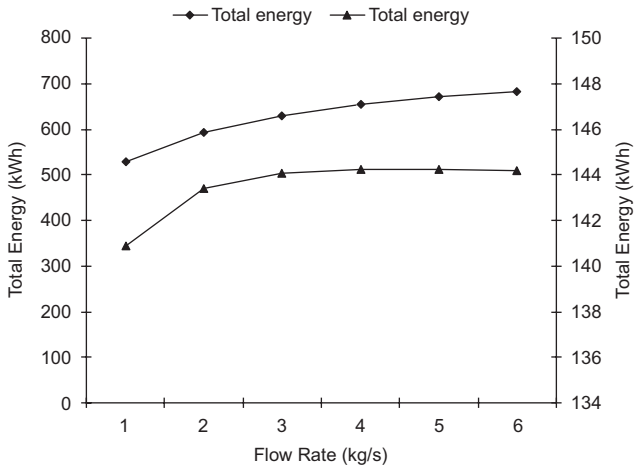

Fig. 8. Total energy (kWh) and exergy (kWh) per annum for different flow rates at Srinagar.

20 W/m^2 at 5 pm to a maximum value of 340 W/m^2 at 12 pm for the month of January (Fig. 5a) where as it varies from a minimum value of 100 W/m^2 at 5 pm to a maximum value of 270 W/m^2 at 1 pm for the month of June (Fig. 5b). The variation in exergy efficiency as shown in Figs. 6 lies between 12% and 15% for the month of January and 13% and 14% for the month of June which is very close to the results obtained by Bosanac et al. [1]. The total exergy varies from a minimum value of 5 W/m^2 at 5 pm to a maximum value of 80 W/m^2 at 12 pm for the month of January (Fig. 6a) where as it varies from a minimum value of 28 W/m^2 at 8 am and 5 pm to a maximum value of 65 W/m^2 at 1 pm for the month of June (Fig. 6b). The variation in electrical output has been evaluated as shown in the numerator of Eq. (11).

The similar calculations were carried out for each case for each month and the total monthly useful energy and exergy were obtained and the results have been shown in Fig. 7. One can observe that the monthly total energy varies between 35 and 65 kWh and corresponding exergy varies between 8 and 15 kWh. This reduction is due to use of second law of thermodynamics in exergy analysis. The monthly energy and exergy are maximum (65 and 15 kWh, respectively) in the month of May and minimum (35 and 8 kWh, respectively) in the month of December; this is due to the more number of clear days available in the month of May as compared to the month of December (Table 4).

Effect of flow rate on yearly energy and exergy in the terms of kWh has been shown in Fig. 8. It shows that the energy and exergy increases with increase of flow rate due to faster use of thermal energy available with PV module as expected. However there is significant decrease in exergy due to more heat losses from the system during use of thermal energy.

4. Conclusions

On the basis of present analysis it is clear that there is an increase of about 2–3% exergy due to thermal energy in addition to its 12% electrical output from PV/T system, which makes an overall electrical efficiency of about 14–15% of PV/T system.

Acknowledgements

The authors are grateful to the Indian Meteorology Department (IMD), Pune, India for providing the hourly global and diffuse radiation and ambient temperature data for Srinagar for four years (1998–2001).

References

[1] Bosanac M, Sorensen B, Ivan K, Sorensen H, Bruno N, Jamal B. Photovoltaic/thermal solar collectors and their potential in Denmark. Final Report, EFP Project 2003, 1713/00-0014. www.solenergi.dk/rapporter/pvtpotentialindenmark.pdf
[2] Coventry SJ, Lovegrove K. Development of an approach to compare the 'value' of electrical and thermal output from a domestic PV/thermal system. Sol Energy 2003;75(1):63–72.
[3] Jones AD, Underwood CP. A thermal model for photovoltaic systems. Sol Energy 2001;70(4):349–59.
[4] Hegazy AA. Comparative study of the performance of four photovoltaic/thermal solar air collectors. Energy Convers Manage 2000;41(8):861–81.
[5] Infield D, Mei L, Eicker U. Thermal performance estimation of ventilated PV facades. Sol Energy 2004; 76(1–3):93–8.
[6] Tripanagnostopoulos Y, Nousia TH, Souliotis M, Yianoulis P. Hybrid photovoltaic/thermal solar system. Sol Energy 2002;72(3):217–34.
[7] Prakash J. Transient analysis of a photovoltaic–thermal solar collector for co-generation of electricity and hot air/water. Energy Convers Manage 1994;35:967–72.
[8] Cartmell BP, Shankland NJ, Fiala D, Hanby V. A multi-operational ventilated photovoltaic and solar air collector: application, simulation and initial monitoring feedback. Sol Energy 2004;76: 45–53.
[9] Bhargava AK, Garg HP, Agarwall RK. Study of a hybrid solar system—solar air heater combined with solar cells. Energy Convers Manage 1991;31(5):471–9.
[10] Odeh N, Grassie T, Henderson D, Muneer T. Modelling of flow rate in a photovoltaic-driven roof slate-based solar ventilation air pre heating system. Energy Convers Manage 2005, in press (www.sciencedirect.com).
[11] Vorobiev Yu, Gonzalez-hernandez J, Vorobiev P, Bulat L. Thermal–photovoltaic hybrid system for efficient solar energy conversion. Sol Energy 2005, in press (www.sciencedirect.com).
[12] Tiwari A, Sodha MS, Chandra A, Joshi JC. Performance evaluation of photovoltaic thermal solar air collector for composite climate of India. Sol Energy Mater Sol Cell 2006;90(2):175–89.
[13] Zondag HA, de Vries DW, de van Helden WGJ, van Zolengen RJC, steenhoven AA. The thermal and electrical yield of a PV-thermal collector. Sol Energy 2002;72(2):113–28.
[14] Kalogirou SA. Use of TRYNSYS for modeling and simulation of a hybrid PV–thermal solar system for Cyprus. Renew Energy 2001;23:247–60.
[15] Garg HP, Agarwall RK, Joshi JC. Experimental study on a hybrid photovoltaic thermal solar water heater and its performance prediction. Energy Convers Manage 1994;35:621–33.
[16] Chow TT. Performance analysis of photovoltaic-thermal collector by explicit dynamic model. Sol Energy 2003;75:143–52.
[17] Zakharchenko R, Licea-Jime'nez L, Pe'rez-Garci'a SA, Vorobiev P, Dehesa-Carrasco U, Pe'rez–Robels JF, et al. Photovoltaic solar panel for a hybrid PV/Thermal system. Sol Energy Mater Sol Cell 2004;82(1–2): 253–61.
[18] Sandnes B, Rekstad J. A photovoltaic/thermal (PV/T) collector with a polymer absorber plate: experimental study and analytic model. Sol Energy 2002;72(1):63–73.
[19] Tiwari A, Sodha MS. Performance evaluation of a solar PV/T system: an experimental validation. Sol Energy 2005, in press.
[20] Huang BJ, Lin TH, Hung WC, Sun FS. Performance evaluation of solar photovoltaic/thermal systems. Sol Energy 2001;70(5):443–8.
[21] Sopian K, Liu HT, Kakac S, Veziroglu TN. Performance of a double pass photovoltaic thermal solar collector suitable for solar drying systems. Energy Convers Manage 2000;41(4):353–65.

[22] Coventry SJ. Performance of a concentrating photovoltaic/thermal solar collector. Sol Energy 2005; 78(2):211–22.
[23] Singh HN, Tiwari GN. Evaluation of cloudiness/haziness factor for composite climate. J Energy 2005; 20:1589–601.
[24] Duffie JA, Beckman WA. Solar engineering of thermal processes. New York: Wiley Interscience; 1991.
[25] Tiwari GN. Solar energy: fundamentals, design modeling and applications. New York and New Delhi: CRC Press and Narosa Publishing House; 2002.
[26] Moran MJ. Engineering thermodynamics. LLC: CRC Press; 1999.